AD-A233 057

NASA Contractor Report 187500
ICASE Report No. 91-6

ICASE

ON THE EFFECTS OF VISCOSITY ON THE STABILITY OF A TRAILING-LINE VORTEX

Peter W. Duck
Mehdi R. Khorrami

DTIC
ELECTE
MAR 12 1991
S E D

Contract No. NAS1-18605
January 1991

Institute for Computer Applications in Science and Engineering
NASA Langley Research Center
Hampton, Virginia 23665-5225

Operated by the Universities Space Research Association

National Aeronautics and
Space Administration

Langley Research Center
Hampton, Virginia 23665-5225

DISTRIBUTION STATEMENT A
Approved for public release;
Distribution Unlimited

91 3 08 040

ON THE EFFECTS OF VISCOSITY ON THE STABILITY OF A TRAILING-LINE VORTEX

Peter W. Duck[1]
Department of Mathematics
University of Manchester
UNITED KINGDOM
and
Mehdi R. Khorrami
High Technology Corporation
Hampton, VA

ABSTRACT

The linear stability of the Batchelor (1964) vortex is investigated. Particular emphasis is placed on modes found recently in a numerical study by Khorrami (1991). These modes have a number of features very distinct from those found previously for this vortex, including (i) exhibiting small growth rates at large Reynolds numbers and (ii) susceptibility to destabilisation by viscosity. In this paper these modes are described using asymptotic techniques, producing results which compare very favourably with fully numerical results at large Reynolds numbers.

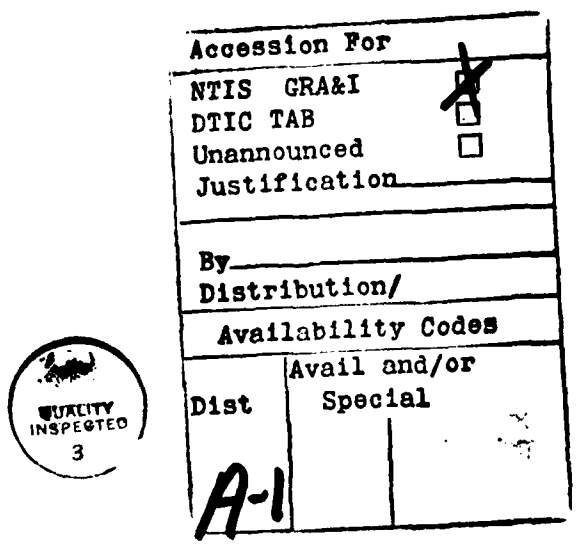

[1]Research was supported by the National Aeronautics and Space Administration under NASA Contract No. NAS1-18605 while the author was in residence at the Institute for Computer Applications in Science and Engineering (ICASE), NASA Langley Research Center, Hampton, VA 23665.

1. Introduction

Stability analysis of streamwise vortices plays an important role in such diverse areas as wake-hazard reduction, combustor optimization, and turbulent boundary-layer structure. Employing the Batchelor vortex (Batchelor 1964) for the mean velocity profile, a great deal of effort has been directed towards understanding the stability characteristics of a trailing-line vortex; the numerical works of Lessen, Singh & Paillet (1974), Lessen & Paillet (1974) and Duck & Foster (1980) should be mentioned. Using asymptotic analysis, the findings of the above authors were confirmed by many investigators, including Stewartson (1982), Leibovich and Stewartson (1983), Stewartson & Capell (1985), Stewartson & Brown (1985), Duck (1986), and Stewartson & Leibovich (1987). These asymptotic studies reveal the complex nature and structures of the inviscid modes with negative azimuthal wavenumbers. Furthermore, they showed the intricacies and difficulties associated with the numerical computations of these instabilities. However, most of the above studies treated only inviscid disturbances, and with the possible exception of the work of Maslowe & Stewartson (1982), viscosity was believed to have a stabilizing influence.

Recently, using a numerical method, Khorrami (1991) found new viscous modes of instability for the Batchelor vortex. The two reported modes are for azimuthal wavenumbers which previously were thought to be stable. Furthermore, Khorrami found these modes differ from the inviscid disturbances studied previously in two respects. First, there are no higher modes associated with them, and second they have growth rates which are generally orders of magnitude smaller. In light of the above, it seems quite unlikely for these new instabilities to have structures similar to the inviscid perturbations reported by previous investigators. However, regarding these

modes, numerical methods are not the proper tool for providing either scale and structural information or a limiting analysis near the neutral curves.

This paper is an effort to address these concerns, as well as to provide firmer grounds for the existence of the instability modes with positive (and zero) azimuthal wavenumbers for the Batchelor vortex. A combination of asymptotic and numerical analysis is presented.

2. Problem Formulation

If (u^*,v^*,w^*) denote the dimensional velocity components in the radial (r^*) azimuthal (θ) and axial (x^*) directions respectively, then the similarity solution of swirling wake flows at high Reynolds numbers due to Batchelor (1964) may be written

$$w_0^* = \frac{C_0}{r^*}(1-e^{-\eta}) \tag{2.1}$$

$$u_0^* = U_0 - \frac{C_0 e^{-\eta}}{8\nu x^*}\log\left[\frac{U_0 x^*}{\nu}\right] + \frac{C_0^2}{8\nu x^*}Q(\eta) - \frac{LU_0^2}{8\nu x^*}e^{-\eta}, \tag{2.2}$$

where $$\eta = \frac{U_0 r^{*2}}{4\nu x^*}, \tag{2.3}$$

ν is the kinematic viscosity of the (incompressible) fluid, L is a constant (akin to a drag coefficient), C_0 is the circulation at large radius, and

$$Q(\eta) = e^{-\eta}\{\log\eta + ei(\eta) - 0.807\} + 2\,ei(\eta) - 2ei(2\eta), \tag{2.4}$$

where

$$ei(\eta) = \int_\eta^\infty \frac{e^{-\zeta}}{\zeta}\,d\zeta. \tag{2.5}$$

Batchelor (1964) showed the term involving $Q(\eta)$ in (2.2) is numerically much smaller in magnitude than the other terms, and consequently will be neglected. Similar assumptions have been implemented by previous studies on the stability of this class of vortical flow, as detailed in the previous section. Following Lessen et al. (1974), we scale velocity by

$$U_s = \frac{C_0^2}{8\nu x^*} \log \frac{U_0 x^*}{\nu} + \frac{L U_0^2}{8\nu x^*}, \tag{2.6}$$

and length scales by

$$r_s = \left[\frac{4\nu x^*}{U_0} \right]^{\frac{1}{2}} . \tag{2.7}$$

This leads to a non-dimensional mean-flow profile given by

$$U = \frac{U_0}{U_s} \cdot e^{-r^2}, \tag{2.8}$$

$$W = \frac{q}{r} (1-e^{-r^2}), \tag{2.9}$$

where
$$q = \frac{C_0}{2\pi U_s r_s} , \tag{2.10}$$

and
$$r = r^*/r_s = \sqrt{\eta}. \tag{2.11}$$

We now write the velocity field as the sum of the mean flow together with a small amplitude perturbation, viz

$$u^* = U_s(U+\delta\tilde{u}),$$

$$v^* = U_s\delta\tilde{v},$$

$$w^* = U_s(W+\delta\tilde{w}), \tag{2.12}$$

whilst the pressure is written as

$$p^* = \rho U_0^2[\Pi+\delta\tilde{p}], \tag{2.13}$$

where

$$\Pi = \frac{C_0^2 U_0}{8\nu x^* U_s^2} Q_1(r), \tag{2.14}$$

with

$$Q_1(r) = \frac{(1-e^{-r^2})}{r} + 2ei(r^2) - 2ei(2r^2). \tag{2.15}$$

A tilde quantity here represents the perturbation about the mean state and δ is the (small) perturbation amplitude. We now make the further assumption that U and W (and indeed also U_0) are independent of x^*. This will generally be an improper assumption, and is equivalent to a parallel flow approximation (which has been used as an

assumption in numerous, diverse, stability investigations previously). However, we justify this step on the following grounds. First, one of the primary aims in this paper is to develop asymptotic theories to compare with previous numerical results, which were all based on the same parallel flow approximation. Second, since to leading order the solutions to which we concern ourselves turn out to be inviscid in form, it can be shown that to first order the parallel flow approximation is a right and proper one.

We now return to consideration of the form to be taken for the perturbation quantities. We write

$$(\tilde{u},\tilde{v},\tilde{w},\tilde{p}) = \{F(r),iG(r),H(r),P(r)\} \quad \exp\{i(\alpha x+n\theta-\alpha ct\}, \tag{2.16}$$

where α and n are the axial and azimuthal wavenumbers respectively, and $c = c_r + i\, c_i$ is the complex wavespeed. It turns out that the problem remains unaltered if we use

$$U = e^{-r^2} \tag{2.17}$$

as the mean axial velocity distribution, provided we also replace "c" by "-c", "W" by "-W" and "P" by "-P". The only net effect of this is on c_r, whilst the important amplification rate c_i is totally unaffected.

If we then substitute (2.12), (2.13), and (2.16) into the equations of motion, and consider terms solely of $O(\delta)$, we then obtain

$$G' + \frac{G}{r} + \alpha F + n\,\frac{H}{r} = 0, \tag{2.18}$$

$$- i\,\frac{G''}{R_e} - \frac{iG'}{R_e r} + \left[\frac{i}{R_e}\left\{\frac{n^2+1}{r^2} + \alpha^2\right\} - \varphi\right]G$$

$$+ \left[\frac{2in}{R_e r^2} - \frac{2W}{r}\right] H + P' = 0, \tag{2.19}$$

$$-\frac{H''}{R_e} - \frac{1}{R_e r} H' + \left[i\varphi + \frac{1}{R_e} \left\{ \frac{n^2+1}{r^2} + \alpha^2 \right\} \right] H$$

$$+ \left[i \frac{dW}{dr} + i \frac{W}{r} + \frac{2n}{R_e r^2} \right] G + i \frac{nP}{r} = 0, \qquad (2.20)$$

$$-\frac{F''}{R_e} - \frac{1}{R_e r} F' + \left[i\varphi + \frac{1}{R_e} \left\{ \frac{n^2}{r^2} + \alpha^2 \right\} \right] F$$

$$+ i \frac{dU}{dr} G + i\alpha P = 0, \qquad (2.21)$$

where a prime denotes differentiation with respect to the radial coordinate. Here the Reynolds number is defined as

$$R_e = \frac{U_s r_s}{\nu}, \qquad (2.22)$$

and

$$\varphi = \alpha(U-c) + \frac{nW}{r}. \qquad (2.23)$$

The boundary conditions that must be imposed on this system are:

at $r = 0$,

$$\text{for } n = 0, \quad G(0) = H(0) = F'(0) = P'(0) = 0,$$

$$\text{for } n = \pm 1, \quad G'(0) = G(0) \pm H(0) = F(0) = P(0) = 0,$$

$$\text{for } n > 1, \quad F(0) = G(0) = H(0) = P(0) = 0, \qquad (2.24)$$

whilst as $r \to \infty$,

$$F(r), G(r), H(r), P(r) \to 0. \qquad (2.25)$$

In the following sections we study the above system in the limit as $R_e \to \infty$.

3. The general leading order behaviour as $R_e \to \infty$

A number of papers previously addressed the inviscid limit of the system (2.18) - (2.21), (2.24), (2.25), in particular for modes which exhibit finite temporal growth rates (αc_i) in this limit. Rather than concern ourselves with these modes, we focus on another family of modes found numerically by Khorrami (1991). These exhibit significantly diminishing growth rates with a decrease in viscosity. Inspection of a number of these results, and others not reported, suggests the following two general characteristics of these modes as $R_e \to \infty$: (i) $c_r = O(1)$ and (ii) $c_i = O(R_e^{-1})$. These trends strongly suggest we seek an asymptotic expansion to our solution of the form

$$\{F,G,H,P\} = \{F_0,G_0,H_0,P_0\} + R_e^{-1}\{F_1,G_1,H_1,P_1\} + O(R_e^{-2}), \quad (3.1)$$

$$c = c_0 + R_e^{-1}\, c_1 + O(R_e^{-2}), \quad (3.2)$$

where we expect c_0 to be real. Substituting (3.1), (3.2) into (2.18)-(2.21) and taking just $O(1)$ terms yields the following (inviscid) system of equations

$$G_0' + \frac{G_0}{r} + \alpha F_0 + \frac{nH_0}{r} = 0, \quad (3.3)$$

$$\varphi_0 G_0 + 2\frac{WH_0}{r} = P_0', \quad (3.4)$$

$$\varphi_0 F_0 + U'G_0 = -\alpha P_0, \quad (3.5)$$

$$\varphi_0 H_0 + (W' + \frac{W}{r})G_0 = -\frac{nP_0}{r}, \quad (3.6)$$

where $$\varphi_0 = \alpha(U - c_0) + \frac{nW}{r}. \quad (3.7)$$

Indeed, F_0 and H_0 may be eliminated between these equations to yield the following ordinary differential equations as determined by Duck and Foster (1980):

$$\frac{dG_0}{dr} = \left[\frac{n(rW)' + \alpha r^2 U'}{r^2\varphi_0} - \frac{1}{r} \right] G_0 + \frac{n^2+\alpha^2 r^2}{r^2\varphi_0} P_0, \quad (3.8)$$

or symbolically

$$L_1 \{G_0, P_0\} = 0, \tag{3.9}$$

together with

$$\frac{dP_0}{dr} = \left[\varphi_0 - \frac{(W^2 r^2)'}{r^3 \varphi_0} \right] G_0 - \frac{2nW}{r^2 \varphi_0} P_0, \tag{3.10}$$

or symbolically

$$L_2 \{G_0, P_0\} = 0. \tag{3.11}$$

The boundary conditions may be simply inferred from (2.24) and (2.25).

Equations (3.8), (3.10) (and equivalent) have been investigated by a number of authors (e.g. Lessen et al 1974, Duck & Foster 1980), in particular for complex values of the wavespeed c_0. For this study, we carried out a similar investigation but sought <u>real</u> values of c_0.

A Chebyshev spectral collocation method was employed to perform the numerical tasks throughout this study, since spectral techniques are well known for their accuracy and fast convergence rate. The mathematical theory of such methods is found in Gottlieb & Orszag (1977) and Gottlieb, Hussaini & Orszag (1984) and is not presented here. Its implementation for the stability of swirling flows is given in detail by Khorrami, Malik & Ash (1989), and readers are referred to that paper for further information. Briefly, the method consists of expanding each perturbation eigenfunction in a truncated Chebyshev series, for example

$$G(\xi) = \sum_{k=0}^{N} a_k T_k(\xi), \tag{3.12}$$

where ξ is the independent variable in Chebyshev space. The governing equations (3.3 and (3.6), in discretized form, are then arranged in a generalized eigenvalue format. That is if D and E represent the coefficient matrices, then

$$D\hat{X} = \omega E\hat{X}, \tag{3.13}$$

where the frequency $\omega = \alpha c$ is the eigenvalue, and the eigenvector $\bar{X}$ is represented by

$$\bar{X} = [G\ H\ F\ P]^T. \qquad (3.14)$$

It should be realized that E is a singular matrix. The singularity is removed by addition of the term $\gamma\omega p$ (which is called an artificial compressibility factor) to the continuity equation (see Malik & Poll 1985), where γ is a small parameter of the order of 10^{-18}. The effect of this on the computed physical eigenvalues is negligible as reported by Khorrami et al. (1989). The method is global and therefore the entire eigenvalue spectrum is obtained in a single run. The complex generalized eigenvalue solver employed is the IMSL QZ routine 'EIGZC'.

The outer boundary conditions were enforced at $r_{max} = 100$, and the number of Chebyshev Polynomials required varied depending on flow conditions, but usually was in the range between 60 and 80. At each step, care was taken to ensure that results were at least six or seven significant figures accurate. The eigenfunctions were obtained using an inverse Rayleigh's method (see Wilkinson 1965). The discretization for the local scheme was also spectral; actually, the same matrices D and E were used to compute the eigenfunctions.

Since it turns out that results from this study for $n = 0$ are somewhat different from those of $n \neq 0$, this has important implications on the asymptotic structure of the solution. Consequently, we shall consider the axisymmetric case separately.

4. Axisymmetric (n=0) modes

For $n = 0$, our numerical scheme produced results for wavespeed c_0 over a range of values of swirl parameter q and axial wavenumber α, which had the following general features: (i) a number of distinct, real modes exist, (ii) all these modes have $c_0 < 0$, and (iii) these modes were quite distinct from those of other studies (e.g. Lessen et al. 1974, Duck & Foster 1980), for which $c_i \neq 0$. Indeed our routine was able to generate these other modes, which served as a useful check on the accuracy of our scheme. Results for c_0 for the case $n = 0$, $q = 1.0$, over a range of α are presented in Fig.1 where two distinct modes are shown. We believe these to be the two most important/dominant in this case. We refer to the mode represented by a solid line as mode I, and that represented by a broken line as mode II.

Note that the significance of $c_0 < 0$ is that no critical layers exist (i.e. $\varphi_0 \neq 0$ for all r), a feature that does lead to certain simplifications.

The key question now is whether these modes are stable or unstable, since the study so far only reveals them to be neutrally stable in the limit of large Reynolds numbers. To determine the effects of viscosity on these modes, we must consider terms $O(R_e^{-1})$ in (2.18) - (2.21). After some algebra, we obtain the following two first order equations for G_1 and P_1:

$$L_1(G_1, P_1) = R_a, \tag{4.1}$$

$$L_2(G_1, P_1) = R_b. \tag{4.2}$$

We may write

$$R_a = R_{a_1} + ic_1 R_{a_2},$$

$$R_b = R_{b_1} + ic_1 R_{b_2}, \tag{4.3}$$

where $R_{a_1} = -\frac{nR_3}{r\varphi_0} - \frac{\alpha R_1}{\varphi_0}$,

$$R_{b_1} = -R_2 + \frac{2W}{r\varphi_0} R_3, \tag{4.4}$$

$$R_{a_2} = -\frac{\alpha}{\varphi_0}\left[\frac{nH_0}{r} + \alpha F_0\right], \tag{4.5}$$

$$R_{b_2} = -\alpha\left[G_0 - \frac{2W}{r\varphi_0} H_0\right], \tag{4.6}$$

where

$$R_1 = -F_0'' - \frac{1}{r} F_0' + \left(\frac{n^2}{r^2} + \alpha^2\right)F_0, \tag{4.7}$$

$$R_2 = -G_0'' - \frac{1}{r} G_0' + \left[\frac{n^2+1}{r^2} + \alpha^2\right]G_0 + \frac{2n}{r^2} H_0, \tag{4.8}$$

$$R_3 = -H_0'' - \frac{1}{r} H_0' + \left[\frac{n^2+1}{r^2} + \alpha^2\right]H_0 + \frac{2n}{r^2} G_0. \tag{4.9}$$

Here we retain n since these equations are also useful for other values of n.

In order that (4.1), (4.2) have a solution, with boundary conditions given by (2.24), (2.25), we must have

$$c_1 = \frac{-i\int_0^\infty \left[G^+ R_{a_1} + P^+ R_{b_1}\right]dr}{\int_0^\infty \left[G^+ R_{a_2} + P^+ R_{b_2}\right]dr}, \tag{4.10}$$

where G^+ and P^+ are the functions adjoint to the system (3.8), (3.10), i.e.

$$\frac{dG^+}{dr} = -\left[\frac{n(rW)' + \alpha r^2 U'}{r^2\varphi_0} - \frac{1}{r}\right]G^+ - \left[\varphi_0 - \frac{(W^2r^2)'}{r^3\varphi_0}\right]P^+, \tag{4.11}$$

$$\frac{dP^+}{dr} = -\left[\frac{n^2+\alpha^2r^2}{r^2\varphi_0}\right]G^+ + \frac{2nW}{r^2\varphi_0}P^+, \qquad (4.12)$$

with boundary conditions

$$P^+(0) = G^{+\prime}(0) = 0 \quad \text{if} \quad n = 0,$$

$$P^{+\prime}(0) = G^+(0) = 0 \quad \text{if} \quad n = \pm 1,$$

$$P^+(0) = G^+(0) = 0 \quad \text{if} \quad |n|>1, \qquad (4.13)$$

and $P^+, G^+ \to 0$ as $r \to \infty$, for all n.

Note that due to the nature of the solution for c_0 real, c_1 must be imaginary. The adjoint system (4.11)-(4.12) is discretized similarly as in the case of the governing equations (3.3)-(3.6). However, owing to the non-linear occurence of φ_0 in (4.11) which results in a quadratic term for the frequency, ω, a slightly different approach is taken. Here, the eigenvalues were obtained using a companion matrix method. The method is very straight-forward (see Bridges & Morris 1984 and Khorrami et al. 1989), and involves linearizing the quadratic term by the following transformation:

$$\tilde{P}^+ - \omega P^+ = 0, \qquad (4.14)$$

which leads to a third equation for the adjoint set. For this case, the eigenvector $\bar{X}$ in (3.13) then becomes

$$\bar{X} = [G^+ \; P^+ \; \tilde{P}^+]^T. \qquad (4.15)$$

It must be mentioned that for each computation, the computed eigenvalue spectrum of the adjoint system matched the spectrum associated with the original set i.e. (3.3) - (3.6). This is an independent check on the accuracy and integrity of our results.

To obtain c_1, a Gauss - Chebyshev quadrature is employed to evaluate the integrals of (4.10); the procedure is straightforward. To ensure accurate results, the number of Chebyshev polynomials, N, was increased until c_1 had converged to at least five significant figures. Typically 90 to 100 polynomials were more than sufficient

to obtain the required accuracy. Results for $\omega_i = \mathrm{Im}\left\{\frac{\alpha c_1}{R_e}\right\}$ for the case $n = 0$, $q = 1.0$ are shown on Fig.2 for mode I, for $R_e = 5000$ and 10,000. It is clear that the first of these modes is destabilised over a range of α with the introduction of the effects of viscosity. Meanwhile, the results for ω_i for mode II are shown in Fig.3, and it is clearly seen that viscosity stabilizes this mode. Also shown (on Fig.4) are results for $\omega_i = \mathrm{Im}\{\alpha c_i\}$ for mode I obtained using the fully viscous routine of Khorrami (1991), at the same values of q and Reynolds numbers. We see that the fully viscous results appear to exhibit an upper neutral point which is predicted extremely effectively by our asymptotic results. The growth rate αc_i in the region of the upper neutral point is also predicted accurately by asymptotic theory. However, there is an important point of disagreement between the $R_e \gg 1$ results and those for the full viscous equations, that concerns the nature of αc_i as $\alpha \to 0$. According to our asymptotic theory this quantity approaches a finite value as $\alpha \to 0$, whilst the fully viscous computation predicts a (sharp) drop off at small values of α.

However, this point of disagreement is quite clear. If $|\alpha c_1|$ approaches a constant value as $\alpha \to 0$, then $c_1 = O(1/\alpha)$ as $\alpha \to 0$, and hence a breakdown in the wavespeed expansion (3.2) must occur. Additionally, if $n = 0$, it is also clear that as $\alpha \to 0$, $\varphi \to 0$ (for bounded c) for all r. Specifically this breakdown must occur when $\alpha = O(R_e^{-1})$, and hence we define a scaled axial wavenumber

$$\bar{\alpha} = R_e\, \alpha = O(1). \qquad (4.16)$$

Guided by our previous results as $\alpha \to 0$, and by consideration of the order of magnitude of various terms in the governing equations, for $\bar{\alpha} = O(1)$ we must have

$$F = R_e\, \hat{F}_0(r) + O(1),$$

$$G = \hat{G}_0(r) + O(R_e^{-1}),$$

$$H = R_e \hat{H}_0(r) + O(1),$$

$$P = R_e \hat{P}_0(r) + O(1), \qquad (4.17)$$

and the expansion for the complex wavespeed (3.2) is retained. Substituting (4.17) into (2.18) - (2.21) and implementing (4.16), we obtain to leading order

$$\hat{G}_0' + \frac{\hat{G}_0}{r} + \bar{\alpha}\hat{F}_0 = 0, \qquad (4.18)$$

$$\frac{2W\hat{H}_0}{r} = \hat{P}_{0_r}, \qquad (4.19)$$

$$-\hat{H}_0'' - \frac{1}{r}\hat{H}_0' + \left[-i\bar{\alpha}c_0 + i\bar{\alpha}U + \frac{n^2+1}{r^2} \right] \hat{H}_0$$

$$+ \left[i\frac{dW}{dr} + i\frac{W}{r} \right] \hat{G}_0 = 0, \qquad (4.20)$$

$$-\hat{F}_0'' - \frac{1}{r}\hat{F}_0' + \left[-i\bar{\alpha}c_0 + i\bar{\alpha}U + \frac{n^2}{r^2} \right] \hat{H}_0$$

$$+ i\frac{dU}{dr}\hat{G}_0 + i\bar{\alpha}\hat{P}_0 = 0, \qquad (4.21)$$

where the appropriate boundary conditions may be inferred from (2.24)-(2.25). The above system is then an eigenvalue problem for $c_0(\bar{\alpha})$, and is solved using a simplified form of the viscous routine used by Khorrami (1991). However, owing to the absence of the eigenvalue term in the r-momentum equation, matrix E becomes singular. Here the singularity is removed via a procedure which utilizes row and column operations (see Metcalfe & Orszag 1973). In this procedure, the rank of matrices D and E is reduced first and the eigenvalues are then obtained using the QZ routine. Results for $\mathrm{Im}\{\bar{\alpha}c_0(\bar{\alpha})\}$ are shown in Fig.5 for the case $q = 1.0$, first mode. It is quite clear that a lower neutral point is predicted (at $\bar{\alpha} \simeq 90$), whilst as $\bar{\alpha} \to \infty$, $\mathrm{Im}\{\bar{\alpha}c_0(\bar{\alpha})\} \to 2.3$ approximately. This is in agreement with the values shown on Fig.2 as $\alpha \to 0$. Indeed a routine asymptotic analysis of the system

(4.18) - (4.21) as $\tilde{\alpha} \to \infty$ confirms a correct asymptotic match with the $\alpha = 0(1)$, $\alpha \to 0$ solution.

Thus, to summarise, we are able to predict (using two asymptotic analyses) both the upper and lower neutral points of this particular unstable mode as well as the temporal growth rates of the full viscous equation results (Fig.4). Furthermore, the system (4.18)-(4.21) was also solved for the second (stable) mode, and it was found that this remained stable over the entire range of $\tilde{\alpha}$. It should at this juncture be emphasised, however, that as $\alpha \to 0$, the use of the parallel flow approximation is likely to become increasingly questionable.

In the following section we go on to consider the $n \neq 0$ modes, paying particular attention to cases for which $n = 1$, although there are some similarities with the axisymmetric case, some important and interesting differences also exist.

5. Non-axisymmetric modes

The paper of Khorrami (1991) presents results for an unstable mode (with a growth rate that diminishes as $R_e \to \infty$) for the particular case $n = 1$. In this section we discuss the stability of such an asymmetric disturbance.

We initially follow the same approach as that carried out in the previous sections and apply these methods to the case $n = 1$, $q = 0.7$. Fig.6 shows the variation of c_0 (which again is real) with α, obtained from the solution of (3.8), (3.10). However, below a critical value of α($= \alpha_0$, say), we see $c_0 < 0$, while above this value c_0 becomes positive. We were able to continue the computation of c_0 beyond α_0 using the numerical scheme described in Section 3. However, since $c_0 > 0$, and our numerical results suggested c_0 remained real, a critical layer must be present at any point at which $\varphi_0 = 0$. Hence computation of such modes, according to Lin (1955), must be carried out by extending the computation into complex r space to avoid the singularity in the differential equation. Although our numerical scheme performed extremely well, by its very nature it is not suitable for obtaining solutions off the real r axis. (The authors did attempt a Runge-Kutta scheme for treating (3.8), (3.10), but extremely small grid sizes which required prohibitatively longer computer times, were necessary for adequate resolution of these modes, even for examples for which $c_0 < 0$, i.e. for which no critical layer existed. Further many spurious modes were generated with this technique.) However, analysis below suggests why it may be possible to extend these computations of (3.8), (3.10) into regimes where critical layers may exist without any special modification of the scheme, or numerical difficulties.

Let us initially confine our attention to values of $\alpha < \alpha_0$,

for which the techniques and analysis of the previous section are applicable without modification. In particular, the computed values of ω_i obtained from (4.10) are shown on Fig.7 as points denoted by 0 for the case $n = 1$, $q = 0.7$, and are to be compared with the values of ω_i obtained using the full viscous equation for the same case, at $R_e = 10000$, as presented in Fig.7. The computed and asymptotic values proved to be indistinguishable on the scale shown in Fig.7. It is apparent that we are able to predict, using our asymptotic theory, the location of a lower neutral point (at $\alpha \simeq 0.05$) without the requirement of a further $\alpha \ll 1$ substructure. Agreement between the asymptotic and fully numerical results is excellent up to $\alpha = \alpha_0$, the point to which our asymptotic results extend. Beyond $\alpha = \alpha_0$, the full viscous equations yield values of ω_i which are initially seen to continue to increase but then rapidly drop in value to give an upper neutral point.

For $\alpha > \alpha_0$, it would appear that there are two distinct possibilities to explain this behaviour.

The first, if c_0 remains real, implies that a critical layer exists. However, if we assume that α is just above the critical value α_0, then

$$\alpha = \alpha_0 + \tilde{\alpha}, \tag{5.1}$$

where $|\tilde{\alpha}| \ll \alpha_0$, and $\tilde{\alpha}$ is taken to be positive. As a result we expect

$$c_0 = \tilde{\alpha}\, \tilde{c}_{00} + O(\tilde{\alpha}^2), \tag{5.2}$$

and to be consistant with (3.2), we must have that $\tilde{\alpha} \gg R_e^{-1}$. Suppose that the location of the critical layer is at $r = r_0$, then using the asymptotic form for $U(r)$ and $W(r)$, we must have

$$r_0 \simeq \left[\frac{nq}{\alpha_0 \tilde{\alpha} \tilde{c}_{00}} \right]^{\frac{1}{2}}. \tag{5.3}$$

If this is sufficiently large then as $r \to r_0$, (3.8), (3.10) approximate to

$$\frac{dG_0}{dr} = -\frac{1}{r_0}\left(_0 - \frac{r_0(n^2+\alpha_0^2 r_0^2)}{2n(r-r_0)}\right) P_0, \qquad (5.4)$$

$$\frac{dP_0}{dr} = -\frac{2nq}{r_0^3}(r-r_0)\, G_0 + \frac{P_0}{r-r_0}. \qquad (5.5)$$

Taking this system (and indeed higher order terms that have been neglected) reveals that the solution for G_0 and P_0 are regular about $r = r_0$, i.e.

$$G_0 = \sum_{n=0}^{\infty} G_{0n}\,(r-r_0)^n, \qquad (5.6)$$

$$P_0 = \sum_{n=0}^{\infty} P_{0n}\,(r-r_0)^{n+1}, \qquad (5.7)$$

and hence no critical layer is required. This perhaps explains why we were able to extend our numerical scheme beyond $\alpha = \alpha_0$ without any special modification or difficulties.

However, as α increases, r_0 moves toward the centre of the vortex (r=0). If c_0 remains real, ultimately the presence of a critical layer will become important, in particular its effect will be profound when $r_0 = 0(1)$, implying $\alpha - \alpha_0 = 0(1)$. Perhaps it is this penetration of the critical layer close to the vortex centre that triggers the sharp drop off in growth rate αc_i with α, to yield the upper neutral point as seen in the fully viscous solutions in Fig.7. However, the presence of the critical layer requires that a detour be made into the complex r plane when considering (2.18) - (2.21). According to Lessen et al. 1974 this detour is below the real axis if Real $\{\varphi'(r_0)\} > 0$, and vice versa. Unfortunately, as remarked earlier, our numerical scheme is confined to the real axis, and so we were unable to carry out the computations for our asymptotic structure beyond $\alpha = \alpha_0$ with any degree of certainty.

A second possibility exists, namely that the inviscid solution of (3.8),

(3.10) yields complex stable values of c_0 for $\alpha > \alpha_0$. This stable inviscid decay rate would then counteract the unstable viscous growth rate which could result in a rapid stabilising trend for $\alpha > \alpha_0$. Unfortunately, our numerical scheme was unable to give a categorical vindication of either of these two possibilities.

6. Conclusion

In this paper we have presented asymptotic analyses which describe and indeed confirm the additional modes of instability recently found numerically for the ''trailing-line vortex'' by Khorrami (1991). These modes are very different in nature from those reported previously, being inviscidly neutral, but are clearly shown in this paper to be destabilised by viscosity. Previously reported modes of instability have been generally inviscidly unstable.

Although our investigation has been confined exclusively to the ''trailing-line vortex'', there is no reason why such mechanisms should not operate in the same way for other vortex flows.

Finally, it must be emphasized again that the parallel flow approximation has been employed throughout this paper, and an interesting extension of this work would be to include the effects of non-parallelism.

Acknowledgements

The work of PWD was supported by the National Aeronautics and Space Administration under NASA Contract NAS1-18605 while PWD was in residence at the Institute for Computer Applications in Science and Enginnering, NASA Langley Research Center, Hampton, V A 23665, USA. The work of MRK was supported by the National Aeronautics and Space Administration under NASA Contract NAS1 - 18240.

References

Batchelor, G.K., 1964. J. Fluid Mech. 20, 645.

Bridges, T.J. and Morris, P.J., 1984. J. Comput. Phys. 55, 437.

Duck, P.W., 1981. Z. angew. Math. Phys. 37, 340.

Duck, P.W. and Foster, M.R., 1980. Z. angew. Math. Phys. 31, 523.

Gottlieb, D., Hussaini, M.Y. and Orszag, S.A., 1984. ''Spectral Methods for Partial Differential Equations'', SIAM, p.1.

Gottlieb, D. and Orszag, S.A., 1977. ''Numerical Anlaysis of Spectral Methods,: Theory and Applications, SIAM.

Khorrami, M.R., 1991. J. Fluid Mech., to appear.

Khorrami, M.R., Malik, M.R. and Ash, R.L., 1989, J. Comput. Phys. 81, 206.

Leibovich, S. and Stewartson, K., 1983. J. Fluid Mech. 126, 335.

Lessen, M. and Paillet, F. 1974. J. Fluid Mech. 63, 769.

Lessen, M., Singh, P.J. and Paillet, F., 1974, J. Fluid Mech. 63, 753.

Lin, C.C. 1955 "The Theory of Hydrodynmaic Stability. Cambridge University Press.

Malik, M.R. and Poll D.I.A., 1985, AIAA Journal, 27, 1362.

Maslowe S.A. and Stewartson, 1982. Phys. Fluid. 25, 1517.

Metcalfe, R.W. and Orszag, S.A. 1973 Flow Research Report No.25, Contract N00014 - 72-C-0365.

Stewartson, K. 1982, Phys. Fluid, 25, 1953.

Stewartson, K. and Brown, S.N. 1985, J. Fluid. Mech. 156, 387.

Stewartson, K. and Capell, K.J. Fluid Mech. 156, 369.

Stewartson, K. and Leibovich, S. 1987. J. Fluid Mech. 178, 549.

Wilkinson, J.H. 1965 ''The Algebraic Eigenvalue Problem. Oxford U.P.

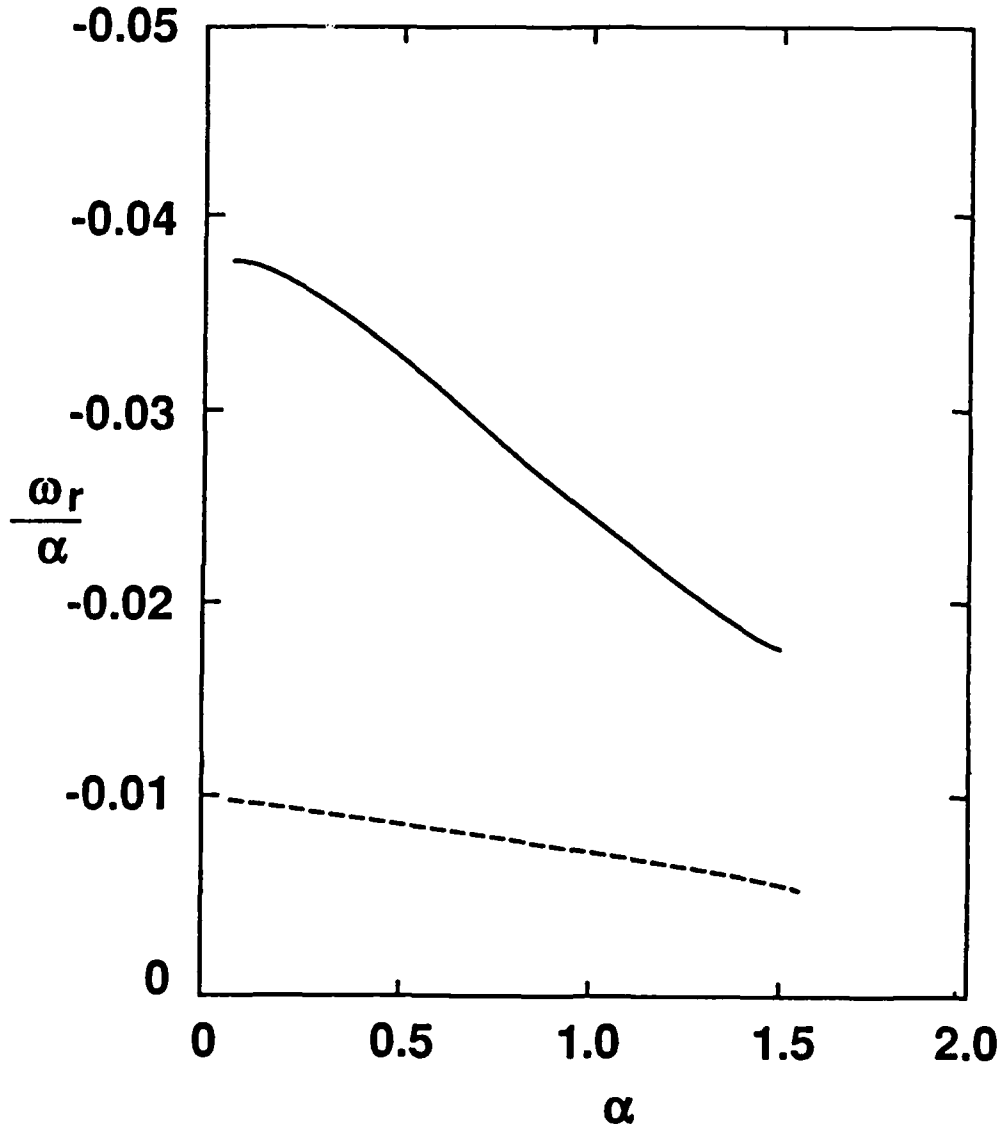

Figure 1. c_0 vs. α, $n = 0$, $q = 1.0$, inviscid calculations, — Mode I, – – – Mode II.

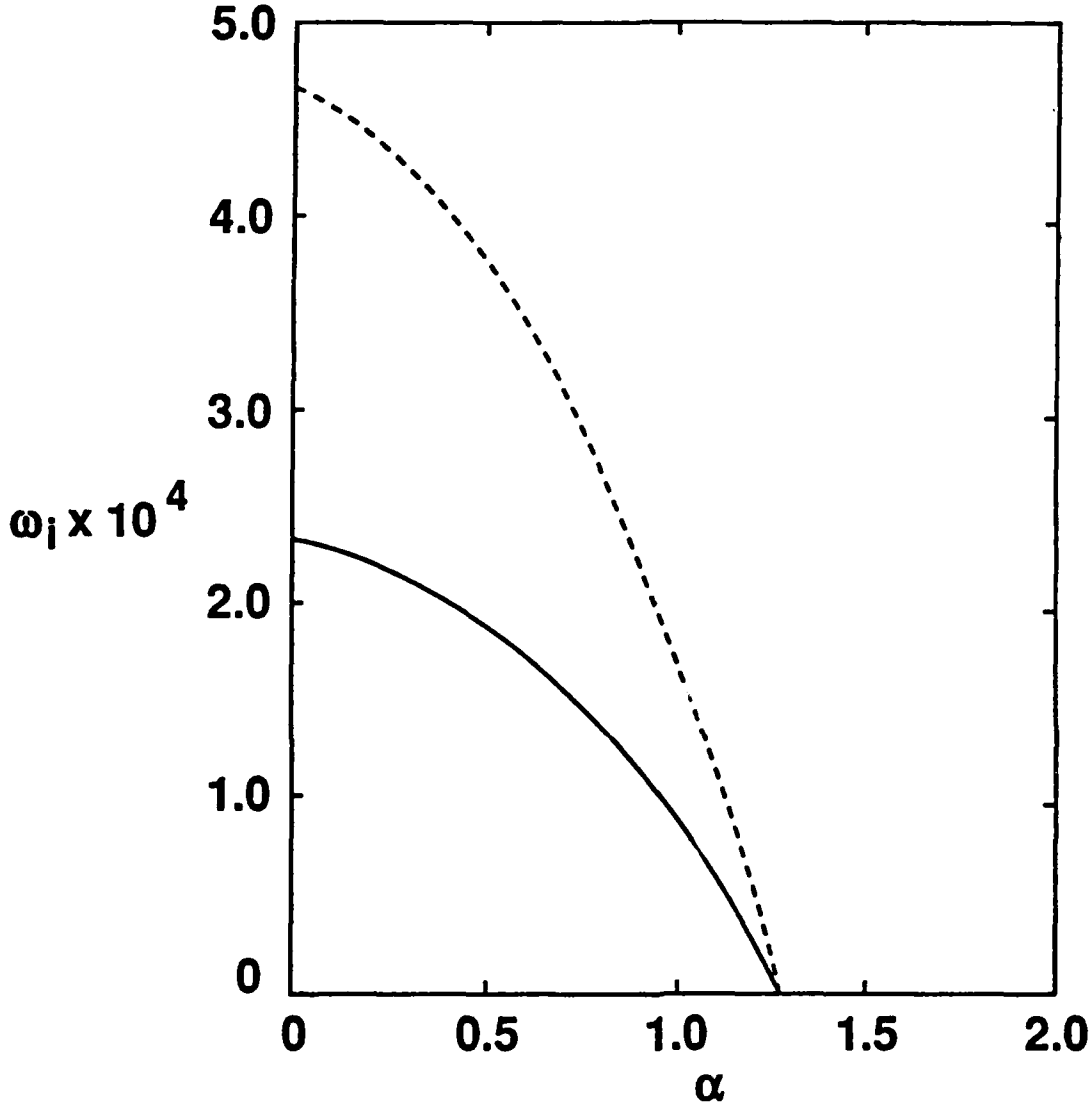

Figure 2. ω_i vs. $\alpha, n = 0, q = 1.0$, asymptotic results, mode I, — $R_e = 10{,}000$, – – – $R_e = 5000$.

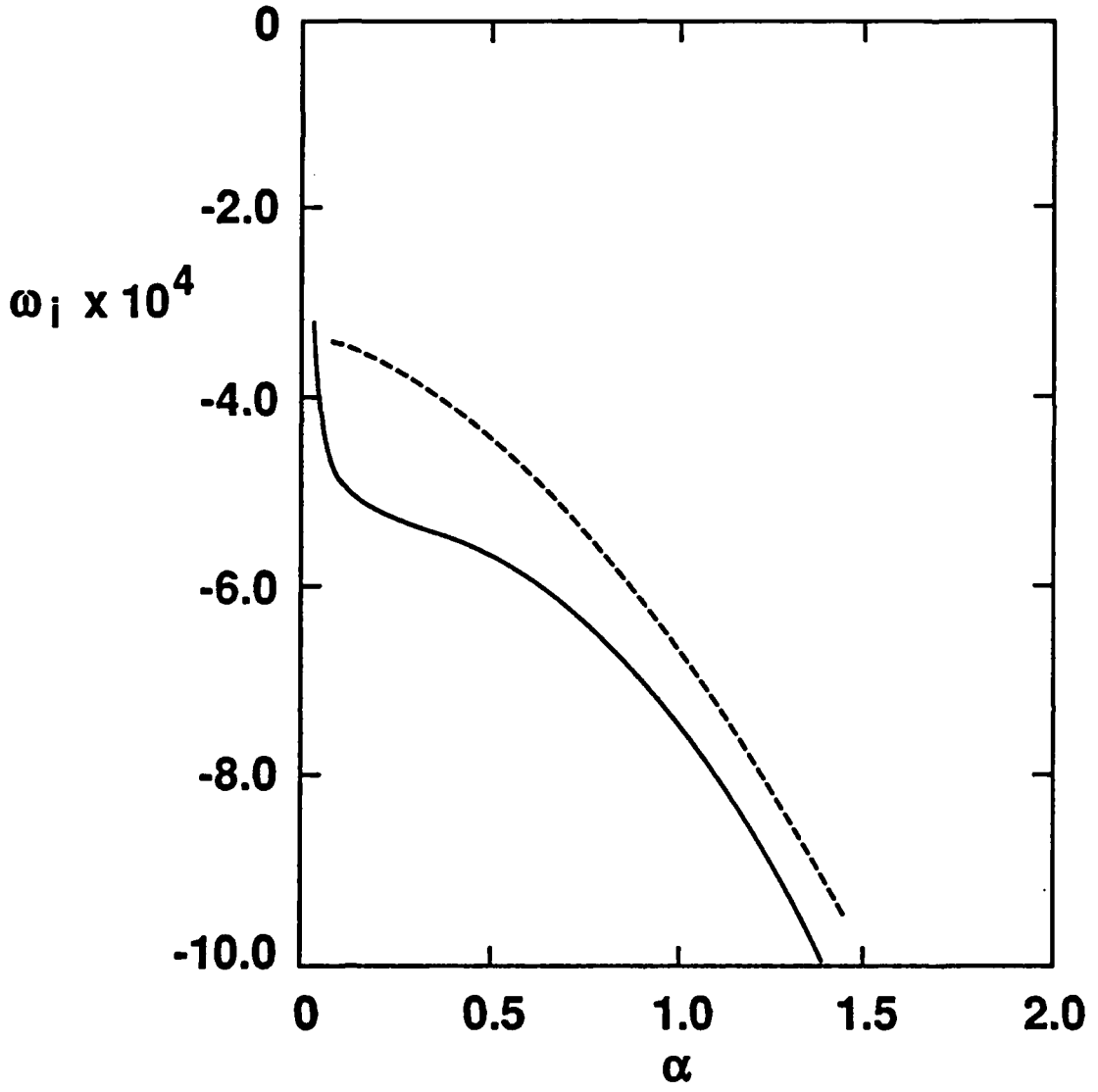

Figure 3. ω_i vs. α, $n = 0$, $q = 1.0$, asymptotic results, $R_e = 10,000$, mode II, — Numerical, – – – Asymptotic.

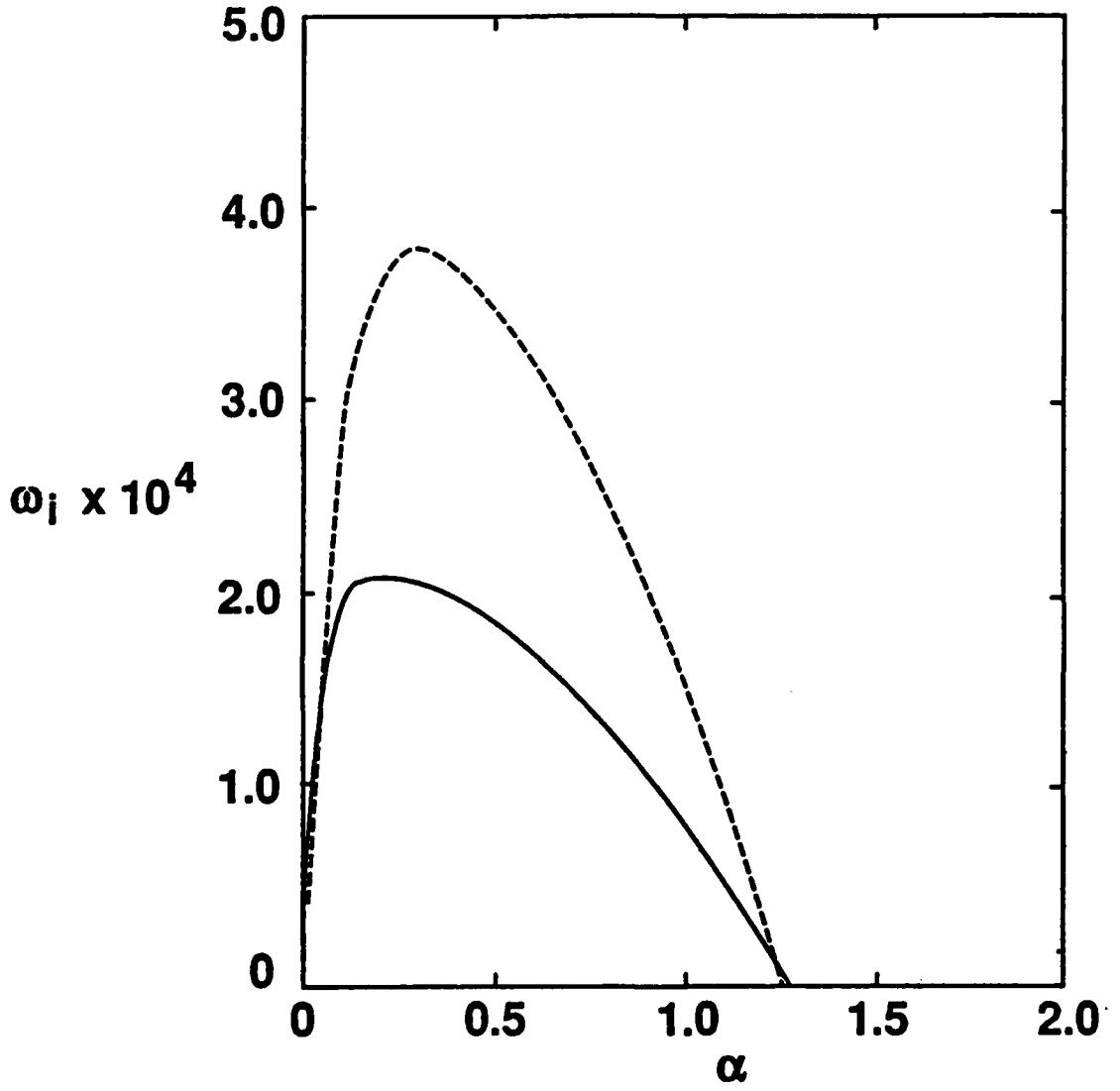

Figure 4. ω_i vs. α, $n = 0$, $q = 1.0$, fully numerical results, — $R_e = 10,000$, – – – $R_e = 5000$.

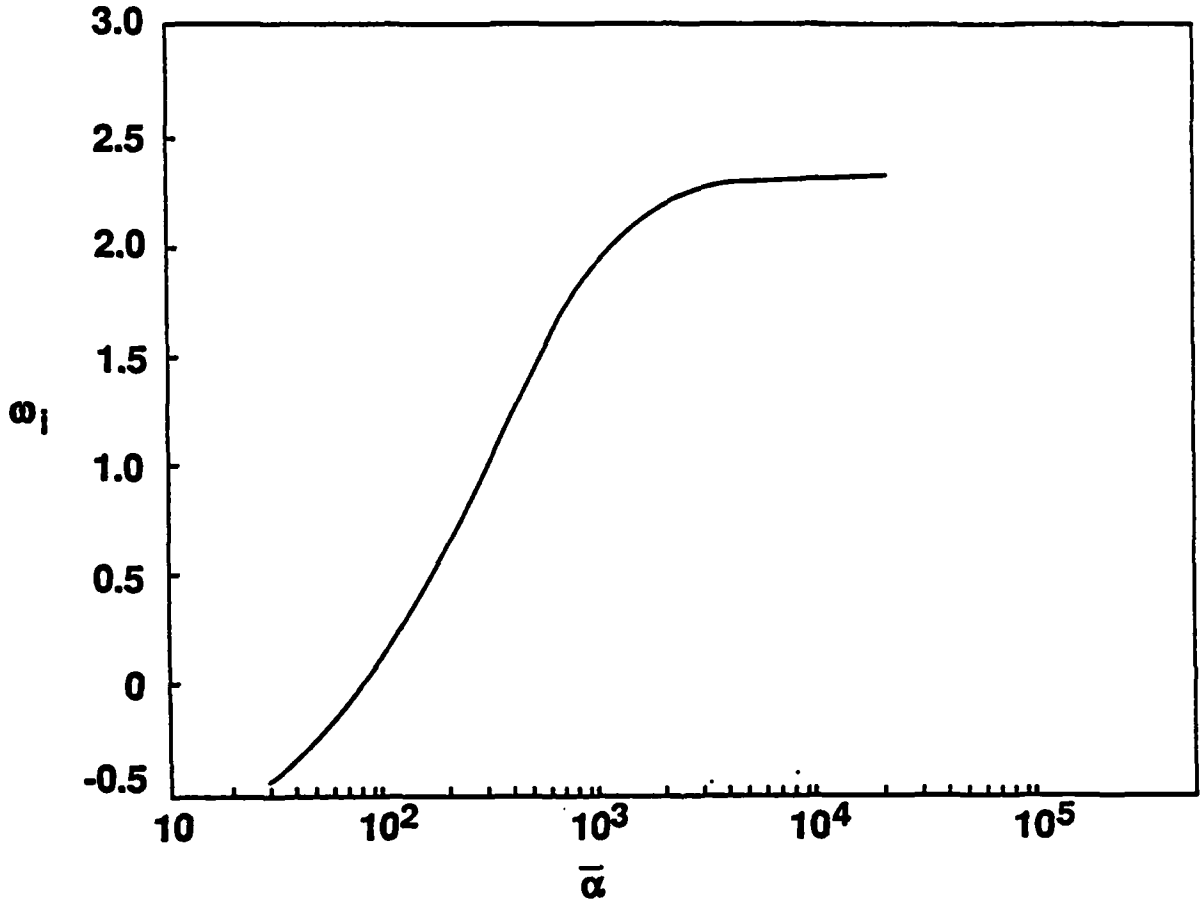

Figure 5. $Im\{\overline{\alpha}c_0(\overline{\alpha})\}$ vs. $\overline{\alpha}$, $n = 0$, $q = 1.0$.

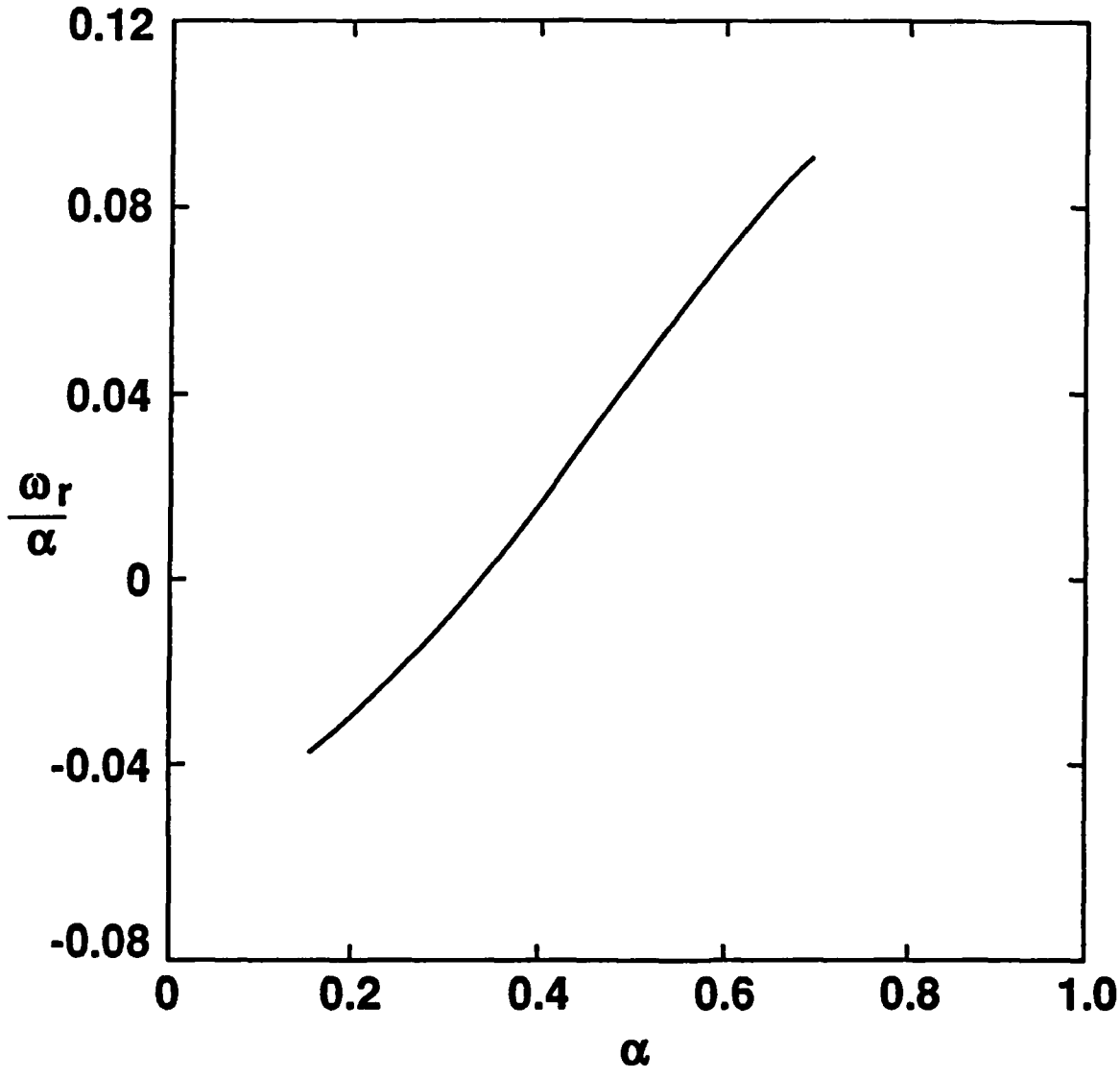

Figure 6. c_0 vs. α, $n = 1$, $q = 0.7$, inviscid calculations.

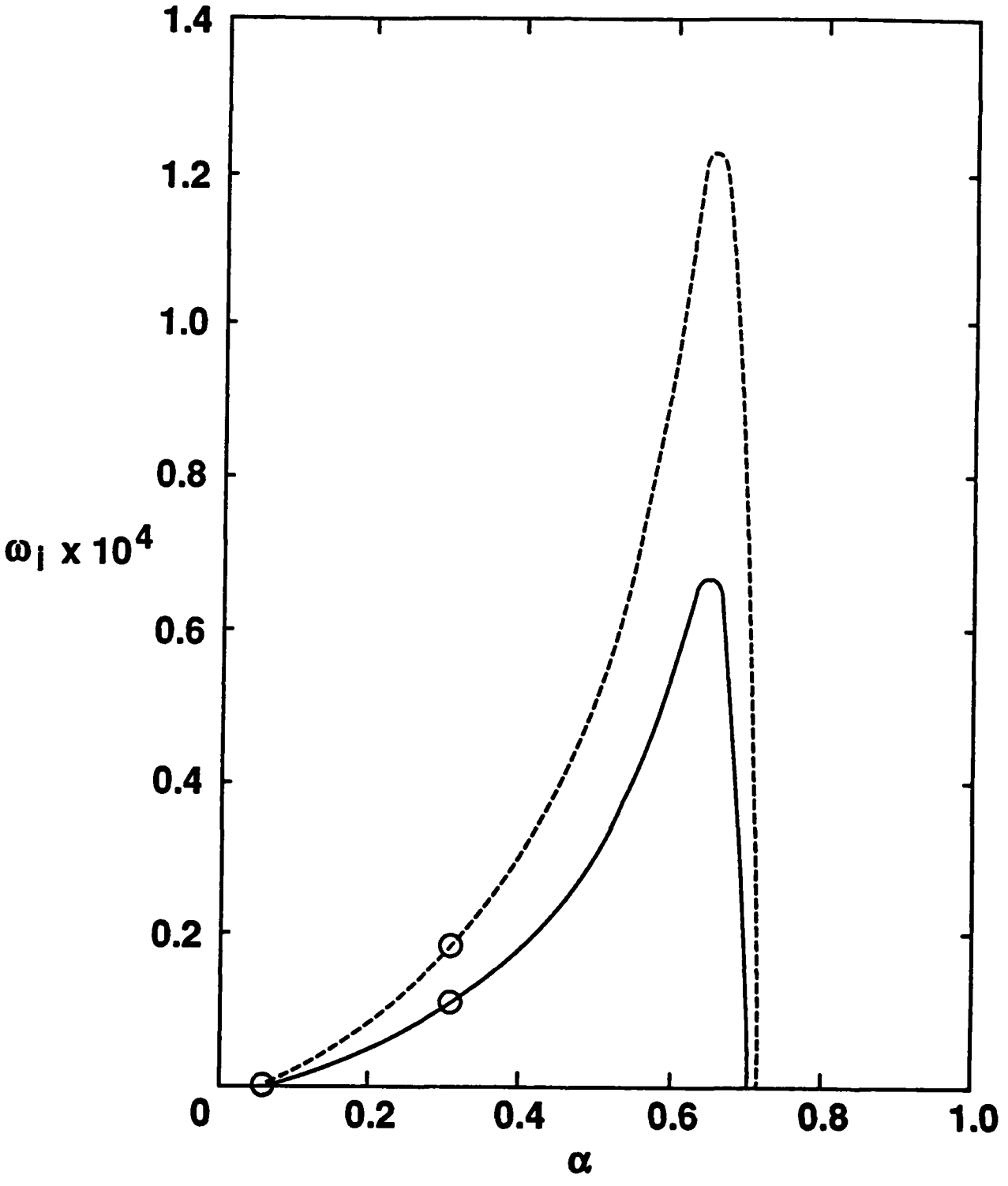

Figure 7. ω_i vs. α, $n = 1$, $q = 0.7$, fully numerical results (circles denote asymptotic points), — $R_e = 10,000$, – – – $R_e = 6000$.